

Topological Phase Transitions

Denjoe O'Connor

Dublin Institute for Advanced Studies

Cardiff, July 2nd 2010

I will describe two very different models where the background geometry and topology under go a phase transition.

Spacetime geometry may not have always existed, it may in fact be an emergent low energy concept. To understand if this is even a possibility one should have some models exhibiting the phenomenon. Furthermore one should understand the class of phase transitions where geometry disappears. Two examples are discussed.

The first part is based on:

- C. Nash and D. O'C., J. Phys **A41** (2009) 012002 [arXiv:0809.2960].

While the 2nd part is based on

- R. Delgadillo-Blando, D. O'C. and B. Ydri, Phys. Rev. Lett. 100,201601 (2008) [arXiv:0712.3011] JHEP05(2009)049 [arXiv:0806.0558]
- C. Nash and D. O'C., J. Phys **A41** (2009) 012002 [arXiv:0809.2960].

The Dimer Model

The dimer model is a classical model in statistical mechanics (see Fisher 1960). It was introduced as a lattice gas of rigid diatomic molecules. Each dimer covers two lattice sites. The simplest model has only hard core interactions with the dimers completely filling the lattice so that there are no monomers (holes).

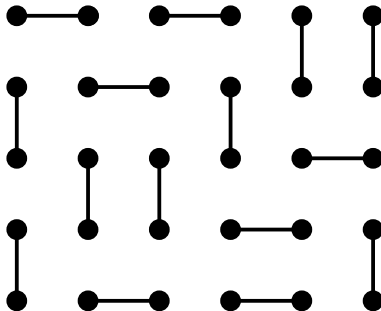
The model can be defined on any graph. Configurations (dimer coverings) are perfect matchings of the graph.

The Dimer Model

The dimer model is a classical model in statistical mechanics (see Fisher 1960). It was introduced as a lattice gas of rigid diatomic molecules. Each dimer covers two lattice sites. The simplest model has only hard core interactions with the dimers completely filling the lattice so that there are no monomers (holes).

The model can be defined on any graph. Configurations (dimer coverings) are perfect matchings of the graph.

Dimer covering of square domain

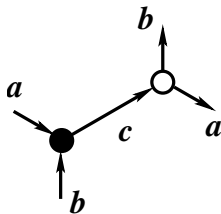


Natural questions arise such as:

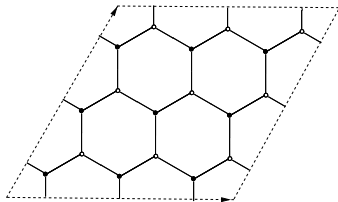
How many dimer coverings are there for a particular graph?

E.g. there are 12988816 perfect matchings
or equivalently domino tilings of a chess board.

Dimer coverings of a hexagonal toroidal lattice



A 3×3 tiling of the torus.



Activities $a = e^{-\beta\epsilon_a}$, $b = e^{-\beta\epsilon_b}$ and $c = e^{-\beta\epsilon_c}$ are assigned to the bonds.

These determine the probability of a bond being active and of a rombus tiling of dual triangular lattice.

The partition function is

$$Z(N, M, a, b, c) = \sum_{\text{tilings}} a^{N_a} b^{N_b} c^{N_c}$$

where N_i is the number of active bonds of type i and $N_a + N_b + N_c = NM$, since the lattice must be completely covered. When the activities are set to one Z counts the number of lozenge tilings of the dual triangular lattice.

By assigning signs judiciously to the adjacency matrix, *Kasteleyn* (*Physica* **27** (1961) 1209-1225) and *Fisher and Temperley* (*Phil. Mag.* **6** (1961) 1061-1063) observed that, one can convert $Z(a, b, c)$ into a Pfaffian of, what is now called, a Kasteleyn matrix.

The “clockwise odd rule” is used: Arrows are placed on the links in such a way that by assigning $+1$ when following an arrow and -1 when opposing one, the product of the signs associated with any fundamental plaquette is -1 when the plaquette is circulated in a counter clockwise direction.

The Kasteleyn matrix element K_{AB} is then given by the activity assigned to the link from vertex A to vertex B times $+1$ if the arrow is from A to B but times -1 if it is from B to A .

A Kasteleyn matrix, K , is therefore a signed weighted adjacency matrix for the lattice. On any simply connected planar domain, the modulus of the Pfaffian of K gives the partition function of the dimer model. $Z = Pfaff(K) = \left| \sqrt{Det(K)} \right|$.

The “clockwise odd rule” is used: Arrows are placed on the links in such a way that by assigning $+1$ when following an arrow and -1 when opposing one, the product of the signs associated with any fundamental plaquette is -1 when the plaquette is circulated in a counter clockwise direction.

The Kasteleyn matrix element K_{AB} is then given by the activity assigned to the link from vertex A to vertex B times $+1$ if the arrow is from A to B but times -1 if it is from B to A .

A Kasteleyn matrix, K , is therefore a signed weighted adjacency matrix for the lattice. On any simply connected planar domain, the modulus of the Pfaffian of K gives the partition function of the dimer model. $Z = Pfaff(K) = \left| \sqrt{Det(K)} \right|$.

On a toroidal lattice the partition function is given by a sum over the different discrete spin structures and therefore involves four terms.

$$Z = \frac{1}{2} \left(-Z_{00} + Z_{\frac{1}{2}0} + Z_{0\frac{1}{2}} + Z_{\frac{1}{2}\frac{1}{2}} \right).$$

Kasteleyn matrices can in fact be viewed as lattice Dirac operators, or more precisely a lattice version of $C\mathcal{D}$ where C is the charge conjugation matrix and \mathcal{D} is the Dirac operator.

In general a Kasteleyn matrix will describe many lattice Fermions with different masses and the theory of classical dimer models is essentially equivalent to that of two dimensional lattice Dirac operators.

On a toroidal lattice the partition function is given by a sum over the different discrete spin structures and therefore involves four terms.

$$Z = \frac{1}{2} \left(-Z_{00} + Z_{\frac{1}{2}0} + Z_{0\frac{1}{2}} + Z_{\frac{1}{2}\frac{1}{2}} \right).$$

Kasteleyn matrices can in fact be viewed as lattice Dirac operators, or more precisely a lattice version of $C\mathcal{D}$ where C is the charge conjugation matrix and \mathcal{D} is the Dirac operator.

In general a Kasteleyn matrix will describe many lattice Fermions with different masses and the theory of classical dimer models is essentially equivalent to that of two dimensional lattice Dirac operators.

On a toroidal lattice the partition function is given by a sum over the different discrete spin structures and therefore involves four terms.

$$Z = \frac{1}{2} \left(-Z_{00} + Z_{\frac{1}{2}0} + Z_{0\frac{1}{2}} + Z_{\frac{1}{2}\frac{1}{2}} \right).$$

Kasteleyn matrices can in fact be viewed as lattice Dirac operators, or more precisely a lattice version of $C\mathcal{D}$ where C is the charge conjugation matrix and \mathcal{D} is the Dirac operator.

In general a Kasteleyn matrix will describe many lattice Fermions with different masses and the theory of classical dimer models is essentially equivalent to that of two dimensional lattice Dirac operators.

On a toroidal lattice the partition function is given by a sum over the different discrete spin structures and therefore involves four terms.

$$Z = \frac{1}{2} \left(-Z_{00} + Z_{\frac{1}{2}0} + Z_{0\frac{1}{2}} + Z_{\frac{1}{2}\frac{1}{2}} \right).$$

Kasteleyn matrices can in fact be viewed as lattice Dirac operators, or more precisely a lattice version of $C\mathcal{D}$ where C is the charge conjugation matrix and \mathcal{D} is the Dirac operator.

In general a Kasteleyn matrix will describe many lattice Fermions with different masses and the theory of classical dimer models is essentially equivalent to that of two dimensional lattice Dirac operators.

Dimer models divide into two classes: Those defined on bipartite and non-bipartite lattices—a lattice is bipartite if its sites can be coloured black and white so that adjacent sites are always of opposite colour. The most general model then assigns a positive number, called an activity, to each bond.

For bipartite dimer models the Kasteleyn matrix takes the form

$$K = \begin{pmatrix} 0 & A \\ -A^T & 0 \end{pmatrix}$$

where A is the black to white links.

Dimer models divide into two classes: Those defined on bipartite and non-bipartite lattices—a lattice is bipartite if its sites can be coloured black and white so that adjacent sites are always of opposite colour. The most general model then assigns a positive number, called an activity, to each bond. For bipartite dimer models the Kasteleyn matrix takes the form

$$K = \begin{pmatrix} 0 & A \\ -A^T & 0 \end{pmatrix}$$

where A is the black to white links.

For the hexagonal 2 site tiling A becomes

$$A_{k_1, k_2; l_1, l_2} = c \delta_{k_1, k_2} \delta_{l_1, l_2} - a \delta_{k_1, k_2+1} \delta_{l_1, l_2} - b \delta_{k_1, k_2} \delta_{l_1, l_2+1}$$

This matrix can be diagonalized using the eigenvectors $z^k w^{-l}$ with $z = e^{\frac{2\pi i n}{N}}$ and $w = e^{\frac{2\pi i n}{N}}$. Then

$$A_{k_1, k_2; l_1, l_2} z^{k_2} w^{-l_2} = (c - a/z - bw) z^{k_1} w^{-l_1}$$

so the eigenvalues are given by the spectral polynomial

$$p^{\text{Hex}}(z, w) = c - a/z - bw .$$

On the torus corresponding to the $N \times M$ covering by the fundamental tile the partition function is given by

$$Z = \frac{1}{2} \sum_{u,v=0}^{1/2} e^{2\pi i(\frac{1}{2}+u+v+2uv)} \text{Det}A_{u,v}$$

with the four terms corresponding to the four discrete spin structures on the torus. For the simple hexagonal lattice

$$\begin{aligned} \text{Det}A_{u,v} &= \prod_{n=0}^{N-1} \prod_{m=0}^{M-1} p^{\text{Hex}} \left(e^{-\frac{2\pi i(n+u)}{N}}, e^{\frac{2\pi i(m+v)}{M}} \right) \\ &= \prod_{m=0}^{M-1} \left(\left(c - b e^{\frac{2\pi i(m+v)}{M}} \right)^N - a^N e^{2\pi i u} \right). \end{aligned}$$

The polynomial $p^{\text{Hex}} = c - \frac{a}{z} - bw$ has two zeros: One at $z = e^{i\Theta}, w = e^{i\Phi}$ the other at $z = e^{-i\Theta}, w = e^{-i\Phi}$.

The counting problem

For the counting problem we want $a = b = c = 1$. Then in the thermodynamic limit $W = \frac{\ln Z}{NM}$,

$$\begin{aligned} W &= \int_0^{2\pi} \frac{d\theta}{2\pi} \int_0^{2\pi} \frac{d\phi}{2\pi} \ln(1 - e^{-i\theta} - e^{i\phi}) \\ &= \frac{1}{\pi} \sum_1^{\infty} \frac{\sin(\frac{n\pi}{3})}{n^2} = \frac{Cl_2(\frac{\pi}{3})}{\pi} \sim 0.323066 \end{aligned}$$

where $Cl_2(x)$ is Clausen's function.

The number of perfect matchings of the hexagonal, toroidal graph

$$\mathcal{N} \sim e^{NM0.323066}$$

There are significant finite size corrections to this result for finite N and M .

The counting problem

For the counting problem we want $a = b = c = 1$. Then in the thermodynamic limit $W = \frac{\ln Z}{NM}$,

$$\begin{aligned} W &= \int_0^{2\pi} \frac{d\theta}{2\pi} \int_0^{2\pi} \frac{d\phi}{2\pi} \ln(1 - e^{-i\theta} - e^{i\phi}) \\ &= \frac{1}{\pi} \sum_1^{\infty} \frac{\sin(\frac{n\pi}{3})}{n^2} = \frac{Cl_2(\frac{\pi}{3})}{\pi} \sim 0.323066 \end{aligned}$$

where $Cl_2(x)$ is Clausen's function.

The number of perfect matchings of the hexagonal, toroidal graph

$$\mathcal{N} \sim e^{NM0.323066}$$

There are significant finite size corrections to this result for finite N and M .

If N and M are positive integral multiples of 6 then $\text{Det}A_{0,0} = 0$ but nonzero otherwise.

A similar structure can be seen for $\text{Det}A_{0,\frac{1}{2}}$, $\text{Det}A_{\frac{1}{2},0}$, $\text{Det}A_{\frac{1}{2},\frac{1}{2}}$.

A careful study of the subleading asymptotics (the finite size corrections) therefore requires that the $N, M \rightarrow \infty$ limit be taken with the mod 6 periodicity in N and M made explicit.

Setting $N = p \bmod 6$ and $M = q \bmod 6$ we obtain

$$\lim_{N, M \rightarrow \infty} \frac{Z(N, M)}{e^{NM \frac{Cl_2(\frac{\pi}{3})}{\pi}}} = \frac{1}{2} \sum_{u, v=0}^{1/2} \left| \frac{\theta\left[\begin{smallmatrix} \theta+u \\ \phi+v \end{smallmatrix}\right](0|\tau)}{\eta(\tau)} \right|$$

with the modular parameter $\tau = \xi e^{\frac{2\pi i}{3}}$, $\xi = \frac{N}{M}$, $\theta = \frac{1}{2} - \frac{q}{6}$ and $\phi = \frac{1}{2} + \frac{p}{6}$.

If $p = q = 0$ this is the conformally invariant partition function for a massless Dirac fermion on the torus with modular parameter

$$\tau = \xi = \frac{N}{M}.$$

If N and M are positive integral multiples of 6 then $\text{Det}A_{0,0} = 0$ but nonzero otherwise.

A similar structure can be seen for $\text{Det}A_{0,\frac{1}{2}}$, $\text{Det}A_{\frac{1}{2},0}$, $\text{Det}A_{\frac{1}{2},\frac{1}{2}}$.

A careful study of the subleading asymptotics (the finite size corrections) therefore requires that the $N, M \rightarrow \infty$ limit be taken with the mod 6 periodicity in N and M made explicit.

Setting $N = p \bmod 6$ and $M = q \bmod 6$ we obtain

$$\lim_{N, M \rightarrow \infty} \frac{Z(N, M)}{e^{NM \frac{Cl_2(\frac{\pi}{3})}{\pi}}} = \frac{1}{2} \sum_{u, v=0}^{1/2} \left| \frac{\theta\left[\begin{smallmatrix} \theta+u \\ \phi+v \end{smallmatrix}\right](0|\tau)}{\eta(\tau)} \right|$$

with the modular parameter $\tau = \xi e^{\frac{2\pi i}{3}}$, $\xi = \frac{N}{M}$, $\theta = \frac{1}{2} - \frac{q}{6}$ and $\phi = \frac{1}{2} + \frac{p}{6}$.

If $p = q = 0$ this is the conformally invariant partition function for a massless Dirac fermion on the torus with modular parameter

$$\tau = \xi = \frac{N}{M}.$$

If N and M are positive integral multiples of 6 then $\text{Det}A_{0,0} = 0$ but nonzero otherwise.

A similar structure can be seen for $\text{Det}A_{0,\frac{1}{2}}, \text{Det}A_{\frac{1}{2},0}, \text{Det}A_{\frac{1}{2},\frac{1}{2}}$.

A careful study of the subleading asymptotics (the finite size corrections) therefore requires that the $N, M \rightarrow \infty$ limit be taken with the mod 6 periodicity in N and M made explicit.

Setting $N = p \bmod 6$ and $M = q \bmod 6$ we obtain

$$\lim_{N, M \rightarrow \infty} \frac{Z(N, M)}{e^{NM \frac{Cl_2(\frac{\pi}{3})}{\pi}}} = \frac{1}{2} \sum_{u, v=0}^{1/2} \left| \frac{\theta\left[\begin{smallmatrix} \theta+u \\ \phi+v \end{smallmatrix} \right](0|\tau)}{\eta(\tau)} \right|$$

with the modular parameter $\tau = \xi e^{\frac{2\pi i}{3}}$, $\xi = \frac{N}{M}$, $\theta = \frac{1}{2} - \frac{q}{6}$ and $\phi = \frac{1}{2} + \frac{p}{6}$.

If $p = q = 0$ this is the conformally invariant partition function for a massless Dirac fermion on the torus with modular parameter

$$\tau = \xi = \frac{N}{M}.$$

If N and M are positive integral multiples of 6 then $\text{Det}A_{0,0} = 0$ but nonzero otherwise.

A similar structure can be seen for $\text{Det}A_{0,\frac{1}{2}}, \text{Det}A_{\frac{1}{2},0}, \text{Det}A_{\frac{1}{2},\frac{1}{2}}$.

A careful study of the subleading asymptotics (the finite size corrections) therefore requires that the $N, M \rightarrow \infty$ limit be taken with the mod 6 periodicity in N and M made explicit.

Setting $N = p \bmod 6$ and $M = q \bmod 6$ we obtain

$$\lim_{N, M \rightarrow \infty} \frac{Z(N, M)}{e^{NM \frac{Cl_2(\frac{\pi}{3})}{\pi}}} = \frac{1}{2} \sum_{u, v=0}^{1/2} \left| \frac{\theta\left[\begin{smallmatrix} \theta+u \\ \phi+v \end{smallmatrix}\right](0|\tau)}{\eta(\tau)} \right|$$

with the modular parameter $\tau = \xi e^{\frac{2\pi i}{3}}$, $\xi = \frac{N}{M}$, $\theta = \frac{1}{2} - \frac{q}{6}$ and $\phi = \frac{1}{2} + \frac{p}{6}$.

If $p = q = 0$ this is the conformally invariant partition function for a massless Dirac fermion on the torus with modular parameter $\tau = \xi = \frac{N}{M}$.

Flat connections

Non zero p and q correspond to a Dirac operator in the presence of flat connections whose holonomies are $e^{i \int_{\gamma} A}$ are $e^{2\pi i \frac{p}{6}}$ and $e^{-2\pi i \frac{q}{6}}$ around the respective nontrivial cycles of the torus.

General weights

For general weights a, b, c and large M and N (the thermodynamic limit) we have the logarithm of the bulk partition function per dimer, $W = \frac{\ln Z}{NM}$, is found to be

$$W(a, b, c) = \int_0^{2\pi} \frac{d\theta}{2\pi} \int_0^{2\pi} \frac{d\phi}{2\pi} \ln(c - ae^{-i\theta} - be^{i\phi}) .$$

If one of the weights is larger than the sum of the other two, then W is the logarithm of that weight. There are three such regions, called frozen regions, where one has $W = \ln a$, $W = \ln b$ and $W = \ln c$.

The region where none of the weights is larger than the sum of the other two is referred to as the amoeba of

the spectral curve

$$p^{\text{Hex}}(z, w) = 1 - \frac{1}{z} - w = 1 - \frac{a}{c}e^{-i\theta} - \frac{b}{c}e^{i\phi}.$$

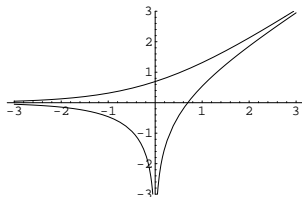
On this curve there are exactly two pairs of angles (Θ, Φ) and $(-\Theta, -\Phi)$ at which $p^{\text{Hex}} = 0$ where,

$$\sin(\Theta) = \frac{b}{2r}, \quad \sin(\Phi) = \frac{a}{2r} \quad \text{and}$$
$$r = \frac{abc}{\sqrt{(a+b+c)(-c+a+b)(c-a+b)(c+a-b)}}.$$

Here, r is the radius of the circumcircle of the triangle with sides a , b and c and opposite angles Φ , Θ and $\pi - \Theta - \Phi$ respectively. The radius r diverges, while Θ and Φ become zero or π , on the boundaries of the amoeba.

The Phase Diagram of the Dimer Model

The phase diagram of a generic bipartite dimer model is given by the amoeba of the spectral polynomial \equiv to the block diagonalization of the lattice Kasteleyn matrix. For the hexagonal lattice the amoeba is:



Then for large M and N we have

$$\begin{aligned} \lim_{N, M \rightarrow \infty} \frac{Z(N, M)}{e^{NMW(a, b, c)}} &= Z_{Dirac}(\tau, \theta, \phi) \\ &= \frac{1}{2} \sum_{u, v=0}^{1/2} \left| \frac{\theta[\frac{\theta+u}{\phi+v}](0|\tau)}{\eta(\tau)} \right| \end{aligned}$$

Where $Z_{Dirac}(\tau, \theta, \phi)$ is the partition function for a Dirac Fermion propagating on the continuum torus with modular parameter τ in the presence of a gauge potential with zero field strength, i.e. a flat connection, but with holonomies $e^{2\pi i\theta}$ and $e^{2\pi i\phi}$ round the cycles of the torus.

The zero of the p^{Hex} occurs at $\Theta = -\frac{2\pi n_0 + \theta}{N}$ and $\Phi = \frac{2\pi m_0 + \phi}{M}$. Then shifting n and m appropriately and expanding around the zero at (Θ, Φ) we have

$$p^{Hex} \simeq -\frac{2\pi ia}{N} e^{-i\Theta} (n + \theta + \tau(m + \phi))$$

where

$$\tau = \frac{Nb}{Ma} e^{i(\Theta + \Phi)} .$$

In the scaling limit, $N, M \rightarrow \infty$, with the activities and $\xi = \frac{N}{M}$ held fixed, τ remains constant and becomes the modular parameter of the continuum limit torus. The second zero at $(-\Theta, -\Phi)$ simply changes τ to $\bar{\tau}$.

On the amoeba the finite size corrections to the dimer model are that of the massless Dirac fermion on the two dimensional torus, with a Dirac operator coupled to flat a connection with non-trivial holonomies around the cycles of the torus.

The torus modular parameter $\tau = \tau_0 + i\tau_1$ is determined by the dimer weights.

As the edge of the amoeba is approached $\tau \rightarrow \tau_0$ and the continuum geometry collapses.

On the amoeba the finite size corrections to the dimer model are that of the massless Dirac fermion on the two dimensional torus, with a Dirac operator coupled to flat a connection with non-trivial holonomies around the cycles of the torus.

The torus modular parameter $\tau = \tau_0 + i\tau_1$ is determined by the dimer weights.

As the edge of the amoeba is approached $\tau \rightarrow \tau_0$ and the continuum geometry collapses.

On the amoeba the finite size corrections to the dimer model are that of the massless Dirac fermion on the two dimensional torus, with a Dirac operator coupled to flat a connection with non-trivial holonomies around the cycles of the torus.

The torus modular parameter $\tau = \tau_0 + i\tau_1$ is determined by the dimer weights.

As the edge of the amoeba is approached $\tau \rightarrow \tau_0$ and the continuum geometry collapses.

Explicitly, for $a = b = e^{-\beta}$ and $c = 1$, for $\beta > \ln 2$ $W = 0$ and for $\beta \leq \ln 2$ we have

$$W = \frac{2}{\pi} \int_{\beta}^{\ln 2} \cos^{-1}\left(\frac{e^y}{2}\right) dy$$

The internal energy $U = -\frac{\partial W}{\partial \beta}$ is continuous throughout the phase diagram while the specific heat $C = \beta^2 \frac{\partial^2 W}{\partial \beta^2}$ diverges at the transition. We have $U = C = 0$, and for $\beta \leq \ln 2$ expanding around $\beta_c = \ln 2$, with $\ln 2 - \beta \geq 0$ we have

$$W(\beta) \simeq \frac{4\sqrt{2}}{3\pi} (\ln 2 - \beta)^{\frac{3}{2}}.$$

$$C \simeq \frac{\sqrt{2}}{\pi} (\ln 2 - \beta)^{-\frac{1}{2}}$$

while

$$\tau \sim \xi \left(1 - 4(\ln 2 - \beta) + i2\sqrt{2}\sqrt{\ln 2 - \beta} \right) + \dots$$

Explicitly, for $a = b = e^{-\beta}$ and $c = 1$, for $\beta > \ln 2$ $W = 0$ and for $\beta \leq \ln 2$ we have

$$W = \frac{2}{\pi} \int_{\beta}^{\ln 2} \cos^{-1}\left(\frac{e^y}{2}\right) dy$$

The internal energy $U = -\frac{\partial W}{\partial \beta}$ is continuous throughout the phase diagram while the specific heat $C = \beta^2 \frac{\partial^2 W}{\partial \beta^2}$ diverges at the transition. We have $U = C = 0$, and for $\beta \leq \ln 2$ expanding around $\beta_c = \ln 2$, with $\ln 2 - \beta \geq 0$ we have

$$W(\beta) \simeq \frac{4\sqrt{2}}{3\pi} (\ln 2 - \beta)^{\frac{3}{2}}.$$

$$C \simeq \frac{\sqrt{2}}{\pi} (\ln 2 - \beta)^{-\frac{1}{2}}$$

while

$$\tau \sim \xi \left(1 - 4(\ln 2 - \beta) + i2\sqrt{2}\sqrt{\ln 2 - \beta} \right) + \dots$$

When the transition is approached on the amoeba the specific heat diverges with exponent $\alpha = \frac{1}{2}$. Off the amoeba the specific heat is constant.

The transition is continuous with no latent heat (or jump in the entropy). The specific heat is zero in the low temperature frozen phase; there is a phase transition at $\beta = \ln 2$, and the specific heat diverges with critical exponent $\alpha = \frac{1}{2}$ as the transition is approached from the high temperature side.

When the transition is approached on the amoeba the specific heat diverges with exponent $\alpha = \frac{1}{2}$. Off the amoeba the specific heat is constant.

The transition is continuous with no latent heat (or jump in the entropy). The specific heat is zero in the low temperature frozen phase; there is a phase transition at $\beta = \ln 2$, and the specific heat diverges with critical exponent $\alpha = \frac{1}{2}$ as the transition is approached from the high temperature side.

The generic bipartite case

The generic bipartite case is described by a spectral polynomial given by $p(z, w) = \text{Det}A(z, w)$. The zero locus of $p(z, w)$ is the spectral curve.

Kenyon and Okounkov proved that the spectral curve, of a $d \times d$ fundamental domain with generic weights is a Harnack curve and furthermore that every Harnack curve arises as the spectral curve of some bipartite dimer model.

Apparently such curves arose in the early twentieth century mathematics literature. They have very special properties and can be characterized by what is referred to as the amoeba of the curve.

The generic bipartite case

The generic bipartite case is described by a spectral polynomial given by $p(z, w) = \text{Det}A(z, w)$. The zero locus of $p(z, w)$ is the spectral curve.

Kenyon and Okounkov proved that the spectral curve, of a $d \times d$ fundamental domain with generic weights is a Harnack curve and furthermore that every Harnack curve arises as the spectral curve of some bipartite dimer model.

Apparently such curves arose in the early twentieth century mathematics literature. They have very special properties and can be characterized by what is referred to as the amoeba of the curve.

The generic bipartite case

The generic bipartite case is described by a spectral polynomial given by $p(z, w) = \text{Det}A(z, w)$. The zero locus of $p(z, w)$ is the spectral curve.

Kenyon and Okounkov proved that the spectral curve, of a $d \times d$ fundamental domain with generic weights is a Harnack curve and furthermore that every Harnack curve arises as the spectral curve of some bipartite dimer model.

Apparently such curves arose in the early twentieth century mathematics literature. They have very special properties and can be characterized by what is referred to as the amoeba of the curve.

General Setting: Matrix Models

Unfortunately, very few multi-matrix models have been solved exactly so far. In contrast one matrix models are quite solvable. To gain some intuition I will review the general features of matrix models.

The Simplest Matrix Model

Consider the Gaussian probability distribution

$$\mathcal{P}(\Phi) = \frac{e^{-\beta \text{Tr}(\Phi^2)}}{Z} \quad \text{where} \quad Z = \int [d\Phi] e^{-\beta \text{Tr}(\Phi^2)} .$$

This distribution splits into the uniform distribution on $M = SU(N)/U(1)^N$ and a probability distribution for the eigenvalues of Φ :

$$\mu(\{\lambda\}) = \prod_{i < j} (\lambda_i - \lambda_j)^2 \frac{e^{-\beta \sum_k \lambda_k^2}}{Z / \text{Vol}(M)} .$$

which for large N converges to the Wigner semi-circle distribution

$$\rho(\lambda) = \frac{\beta}{N\pi} \sqrt{\frac{2N}{\beta} - \lambda^2} .$$

$$\left\langle \frac{\text{Tr}(\Phi^2)}{N} \right\rangle = \int_{-\sqrt{\frac{2N}{\beta}}}^{\sqrt{\frac{2N}{\beta}}} \lambda^2 \rho(\lambda) d\lambda = \frac{N}{2\beta} .$$

The Simplest Matrix Model

Consider the Gaussian probability distribution

$$\mathcal{P}(\Phi) = \frac{e^{-\beta \text{Tr}(\Phi^2)}}{Z} \quad \text{where} \quad Z = \int [d\Phi] e^{-\beta \text{Tr}(\Phi^2)} .$$

This distribution splits into the uniform distribution on $M = SU(N)/U(1)^N$ and a probability distribution for the eigenvalues of Φ :

$$\mu(\{\lambda\}) = \prod_{i < j} (\lambda_i - \lambda_j)^2 \frac{e^{-\beta \sum_k \lambda_k^2}}{Z / \text{Vol}(M)} .$$

which for large N converges to the Wigner semi-circle distribution

$$\rho(\lambda) = \frac{\beta}{N\pi} \sqrt{\frac{2N}{\beta} - \lambda^2} .$$

$$\left\langle \frac{\text{Tr}(\Phi^2)}{N} \right\rangle = \int_{-\sqrt{\frac{2N}{\beta}}}^{\sqrt{\frac{2N}{\beta}}} \lambda^2 \rho(\lambda) d\lambda = \frac{N}{2\beta} .$$

The Simplest Matrix Model

Consider the Gaussian probability distribution

$$\mathcal{P}(\Phi) = \frac{e^{-\beta \text{Tr}(\Phi^2)}}{Z} \quad \text{where} \quad Z = \int [d\Phi] e^{-\beta \text{Tr}(\Phi^2)} .$$

This distribution splits into the uniform distribution on $M = SU(N)/U(1)^N$ and a *probability distribution* for the eigenvalues of Φ :

$$\mu(\{\lambda\}) = \prod_{i < j} (\lambda_i - \lambda_j)^2 \frac{e^{-\beta \sum_k \lambda_k^2}}{Z/\text{Vol}(M)} .$$

which for large N converges to the Wigner semi-circle distribution

$$\rho(\lambda) = \frac{\beta}{N\pi} \sqrt{\frac{2N}{\beta} - \lambda^2} .$$

$$\left\langle \frac{\text{Tr}(\Phi^2)}{N} \right\rangle = \int_{-\sqrt{\frac{2N}{\beta}}}^{\sqrt{\frac{2N}{\beta}}} \lambda^2 \rho(\lambda) d\lambda = \frac{N}{2\beta} .$$

The Simplest Matrix Model

Consider the Gaussian probability distribution

$$\mathcal{P}(\Phi) = \frac{e^{-\beta \text{Tr}(\Phi^2)}}{Z} \quad \text{where} \quad Z = \int [d\Phi] e^{-\beta \text{Tr}(\Phi^2)} .$$

This distribution splits into the uniform distribution on $M = SU(N)/U(1)^N$ and a *probability distribution* for the eigenvalues of Φ :

$$\mu(\{\lambda\}) = \prod_{i < j} (\lambda_i - \lambda_j)^2 \frac{e^{-\beta \sum_k \lambda_k^2}}{Z/\text{Vol}(M)} .$$

which for large N converges to the Wigner semi-circle distribution

$$\rho(\lambda) = \frac{\beta}{N\pi} \sqrt{\frac{2N}{\beta} - \lambda^2} .$$

$$\left\langle \frac{\text{Tr}(\Phi^2)}{N} \right\rangle = \int_{-\sqrt{\frac{2N}{\beta}}}^{\sqrt{\frac{2N}{\beta}}} \lambda^2 \rho(\lambda) d\lambda = \frac{N}{2\beta} .$$

The Simplest Matrix Model

Consider the Gaussian probability distribution

$$\mathcal{P}(\Phi) = \frac{e^{-\beta \text{Tr}(\Phi^2)}}{Z} \quad \text{where} \quad Z = \int [d\Phi] e^{-\beta \text{Tr}(\Phi^2)} .$$

This distribution splits into the uniform distribution on $M = SU(N)/U(1)^N$ and a *probability distribution* for the eigenvalues of Φ :

$$\mu(\{\lambda\}) = \prod_{i < j} (\lambda_i - \lambda_j)^2 \frac{e^{-\beta \sum_k \lambda_k^2}}{Z/\text{Vol}(M)} .$$

which for large N converges to the Wigner semi-circle distribution

$$\rho(\lambda) = \frac{\beta}{N\pi} \sqrt{\frac{2N}{\beta} - \lambda^2} .$$

$$\left\langle \frac{\text{Tr}}{N}(\Phi^2) \right\rangle = \int_{-\sqrt{\frac{2N}{\beta}}}^{\sqrt{\frac{2N}{\beta}}} \lambda^2 \rho(\lambda) d\lambda = \frac{N}{2\beta} .$$

Generic Features of Random Matrix models.

Random matrix models, of a single random matrix, are typically characterised by the eigenvalue distribution of the random matrix.

They have the generic features:

- The eigenvalues repel one another.
- The eigenvalues all fall within a finite domain. The domain may not be connected—the distribution is concentrated on “cuts”. For the Wigner semi-circle the cut is $[-\sqrt{\frac{2N}{\beta}}, \sqrt{\frac{2N}{\beta}}]$.
- The spread in eigenvalues grows (typically) as \sqrt{N} .
- Phase transitions occur when cuts merge or separate.

Generic Features of Random Matrix models.

Random matrix models, of a single random matrix, are typically characterised by the eigenvalue distribution of the random matrix. They have the generic features:

- The eigenvalues repel one another.
- The eigenvalues all fall within a finite domain. The domain may not be connected—the distribution is concentrated on “cuts”. For the Wigner semi-circle the cut is $[-\sqrt{\frac{2N}{\beta}}, \sqrt{\frac{2N}{\beta}}]$.
- The spread in eigenvalues grows (typically) as \sqrt{N} .
- Phase transitions occur when cuts merge or separate.

Generic Features of Random Matrix models.

Random matrix models, of a single random matrix, are typically characterised by the eigenvalue distribution of the random matrix. They have the generic features:

- The eigenvalues repel one another.
- The eigenvalues all fall within a finite domain. The domain may not be connected—the distribution is concentrated on “cuts”. For the Wigner semi-circle the cut is $[-\sqrt{\frac{2N}{\beta}}, \sqrt{\frac{2N}{\beta}}]$.
- The spread in eigenvalues grows (typically) as \sqrt{N} .
- Phase transitions occur when cuts merge or separate.

Generic Features of Random Matrix models.

Random matrix models, of a single random matrix, are typically characterised by the eigenvalue distribution of the random matrix. They have the generic features:

- The eigenvalues repel one another.
- The eigenvalues all fall within a finite domain. The domain may not be connected—the distribution is concentrated on “cuts”. For the Wigner semi-circle the cut is $[-\sqrt{\frac{2N}{\beta}}, \sqrt{\frac{2N}{\beta}}]$.
- The spread in eigenvalues grows (typically) as \sqrt{N} .
- Phase transitions occur when cuts merge or separate.

Generic Features of Random Matrix models.

Random matrix models, of a single random matrix, are typically characterised by the eigenvalue distribution of the random matrix. They have the generic features:

- The eigenvalues repel one another.
- The eigenvalues all fall within a finite domain. The domain may not be connected—the distribution is concentrated on “cuts”. For the Wigner semi-circle the cut is $[-\sqrt{\frac{2N}{\beta}}, \sqrt{\frac{2N}{\beta}}]$.
- The spread in eigenvalues grows (typically) as \sqrt{N} .
- Phase transitions occur when cuts merge or separate.

Generic Features of Random Matrix models.

Random matrix models, of a single random matrix, are typically characterised by the eigenvalue distribution of the random matrix. They have the generic features:

- The eigenvalues repel one another.
- The eigenvalues all fall within a finite domain. The domain may not be connected—the distribution is concentrated on “cuts”. For the Wigner semi-circle the cut is $[-\sqrt{\frac{2N}{\beta}}, \sqrt{\frac{2N}{\beta}}]$.
- The spread in eigenvalues grows (typically) as \sqrt{N} .
- Phase transitions occur when cuts merge or separate.

Generic Features of Random Matrix models.

Random matrix models, of a single random matrix, are typically characterised by the eigenvalue distribution of the random matrix. They have the generic features:

- The eigenvalues repel one another.
- The eigenvalues all fall within a finite domain. The domain may not be connected—the distribution is concentrated on “cuts”. For the Wigner semi-circle the cut is $[-\sqrt{\frac{2N}{\beta}}, \sqrt{\frac{2N}{\beta}}]$.
- The spread in eigenvalues grows (typically) as \sqrt{N} .
- Phase transitions occur when cuts merge or separate.

Generic Features of Random Matrix models.

Random matrix models, of a single random matrix, are typically characterised by the eigenvalue distribution of the random matrix. They have the generic features:

- The eigenvalues repel one another.
- The eigenvalues all fall within a finite domain. The domain may not be connected—the distribution is concentrated on “cuts”. For the Wigner semi-circle the cut is $[-\sqrt{\frac{2N}{\beta}}, \sqrt{\frac{2N}{\beta}}]$.
- The spread in eigenvalues grows (typically) as \sqrt{N} .
- Phase transitions occur when cuts merge or separate.

Example: The Φ^4 matrix model.

$V(\Phi) = \text{Tr}(b\Phi^2 + c\Phi^4)$ with Φ an $N \times N$ matrix.

- The model is characterized by the distribution of the eigenvalues of Φ .
- For $c = 0$ the eigenvalues have a Wigner semi-circle distribution.
- For $c > 0$ and $b \ll 0$ the eigenvalues fall into two disconnected regions, i.e. they have a “two cut” distribution.
- The partition is not analytic at $b = -2\sqrt{Nc}$, only the first two derivatives of $\ln Z$ are continuous and the phase transition is of 3rd order.
- The random matrix “gravity” transition occurs for $c < 0$ and $b > 0$.

Example: The Φ^4 matrix model.

$V(\Phi) = \text{Tr}(b\Phi^2 + c\Phi^4)$ with Φ an $N \times N$ matrix.

- The model is characterized by the distribution of the eigenvalues of Φ .
- For $c = 0$ the eigenvalues have a Wigner semi-circle distribution.
- For $c > 0$ and $b \ll 0$ the eigenvalues fall into two disconnected regions, i.e. they have a “two cut” distribution.
- The partition is not analytic at $b = -2\sqrt{Nc}$, only the first two derivatives of $\ln Z$ are continuous and the phase transition is of 3rd order.
- The random matrix “gravity” transition occurs for $c < 0$ and $b > 0$.

Example: The Φ^4 matrix model.

$V(\Phi) = \text{Tr}(b\Phi^2 + c\Phi^4)$ with Φ an $N \times N$ matrix.

- The model is characterized by the distribution of the eigenvalues of Φ .
- For $c = 0$ the eigenvalues have a Wigner semi-circle distribution.
- For $c > 0$ and $b \ll 0$ the eigenvalues fall into two disconnected regions, i.e. they have a “two cut” distribution.
- The partition is not analytic at $b = -2\sqrt{Nc}$, only the first two derivatives of $\ln Z$ are continuous and the phase transition is of 3rd order.
- The random matrix “gravity” transition occurs for $c < 0$ and $b > 0$.

Example: The Φ^4 matrix model.

$V(\Phi) = \text{Tr}(b\Phi^2 + c\Phi^4)$ with Φ an $N \times N$ matrix.

- The model is characterized by the distribution of the eigenvalues of Φ .
- For $c = 0$ the eigenvalues have a Wigner semi-circle distribution.
- For $c > 0$ and $b \ll 0$ the eigenvalues fall into two disconnected regions, i.e. they have a “two cut” distribution.
- The partition is not analytic at $b = -2\sqrt{Nc}$, only the first two derivatives of $\ln Z$ are continuous and the phase transition of 3rd order.
- The random matrix “gravity” transition occurs for $c < 0$ and $b > 0$.

Example: The Φ^4 matrix model.

$V(\Phi) = \text{Tr}(b\Phi^2 + c\Phi^4)$ with Φ an $N \times N$ matrix.

- The model is characterized by the distribution of the eigenvalues of Φ .
- For $c = 0$ the eigenvalues have a Wigner semi-circle distribution.
- For $c > 0$ and $b \ll 0$ the eigenvalues fall into two disconnected regions, i.e. they have a “two cut” distribution.
- The partition is not analytic at $b = -2\sqrt{Nc}$,
only the first two derivatives of $\ln Z$ are continuous and the phase transition of 3rd order.
- The random matrix “gravity” transition occurs for $c < 0$ and $b > 0$.

Example: The Φ^4 matrix model.

$V(\Phi) = \text{Tr}(b\Phi^2 + c\Phi^4)$ with Φ an $N \times N$ matrix.

- The model is characterized by the distribution of the eigenvalues of Φ .
- For $c = 0$ the eigenvalues have a Wigner semi-circle distribution.
- For $c > 0$ and $b \ll 0$ the eigenvalues fall into two disconnected regions, i.e. they have a “two cut” distribution.
- The partition is not analytic at $b = -2\sqrt{Nc}$, only the first two derivatives of $\ln Z$ are continuous and the phase transition of 3rd order.
- The random matrix “gravity” transition occurs for $c < 0$ and $b > 0$.

Example: The Φ^4 matrix model.

$V(\Phi) = \text{Tr}(b\Phi^2 + c\Phi^4)$ with Φ an $N \times N$ matrix.

- The model is characterized by the distribution of the eigenvalues of Φ .
- For $c = 0$ the eigenvalues have a Wigner semi-circle distribution.
- For $c > 0$ and $b \ll 0$ the eigenvalues fall into two disconnected regions, i.e. they have a “two cut” distribution.
- The partition is not analytic at $b = -2\sqrt{Nc}$, only the first two derivatives of $\ln Z$ are continuous and the phase transition is of 3rd order.
- The random matrix “gravity” transition occurs for $c < 0$ and $b > 0$.

A 3-matrix model with $SO(3)$ symmetry.

Consider single trace 3-matrix model with global $SO(3)$ symmetry has energy

$$E = \frac{\text{Tr}}{N} \left(-\frac{1}{4} [D_j, D_k]^2 + \frac{2i}{3} \epsilon_{jkl} D_j D_k D_l \right)$$

$E(D)$ has translational symmetry $D_j \rightarrow D_j + d_j \mathbf{1}$ symmetry.

Partition Function

$$Z(\beta) = \int [dD_j] e^{-S(D)} \quad \text{where} \quad S(D) = -\beta E(D)$$

A 3-matrix model with $SO(3)$ symmetry.

Consider single trace 3-matrix model with global $SO(3)$ symmetry has energy

$$E = \frac{\text{Tr}}{N} \left(-\frac{1}{4} [D_j, D_k]^2 + \frac{2i}{3} \epsilon_{jkl} D_j D_k D_l \right)$$

$E(D)$ has translational symmetry $D_j \rightarrow D_j + d_j \mathbf{1}$ symmetry.

Partition Function

$$Z(\beta) = \int [dD_j] e^{-S(D)} \quad \text{where} \quad S(D) = -\beta E(D)$$

A 3-matrix model with $SO(3)$ symmetry.

Consider single trace 3-matrix model with global $SO(3)$ symmetry has energy

$$E = \frac{\text{Tr}}{N} \left(-\frac{1}{4} [D_j, D_k]^2 + \frac{2i}{3} \epsilon_{jkl} D_j D_k D_l \right)$$

$E(D)$ has translational symmetry $D_j \rightarrow D_j + d_j \mathbf{1}$ symmetry.

Partition Function

$$Z(\beta) = \int [dD_j] e^{-S(D)} \quad \text{where} \quad S(D) = -\beta E(D)$$

Ground State

The critical points of the model are given by

$$[D_k, ([D_j, D_k] - i\epsilon_{jkl}D_l)] = 0.$$

So representations of the Lie algebra of $SU(2)$ are critical points with energy $E_{saddle} = -\frac{1}{6} \frac{\text{Tr}(D_j^2)}{N}$.

The minimum energy configuration is

$$D_j = L_j \text{ with } E_0 = -\frac{N^2-1}{24}.$$

The L_j satisfy

$$[L_j, L_j] = i\epsilon_{jkl}L_l \text{ and } L_j L_j = \frac{N^2-1}{4} \mathbf{1}.$$

These are the familiar commutation relations of angular momentum.

Ground State

The critical points of the model are given by

$$[D_k, ([D_j, D_k] - i\epsilon_{jkl}D_l)] = 0.$$

So representations of the Lie algebra of $SU(2)$ are critical points with energy $E_{saddle} = -\frac{1}{6} \frac{\text{Tr}(D_j^2)}{N}$.

The minimum energy configuration is

$$D_j = L_j \text{ with } E_0 = -\frac{N^2-1}{24}.$$

The L_j satisfy

$$[L_j, L_k] = i\epsilon_{jkl}L_l \text{ and } L_j L_j = \frac{N^2-1}{4} \mathbf{1}.$$

These are the familiar commutation relations of angular momentum.

Ground State

The critical points of the model are given by

$$[D_k, ([D_j, D_k] - i\epsilon_{jkl}D_l)] = 0.$$

So representations of the Lie algebra of $SU(2)$ are critical points with energy $E_{saddle} = -\frac{1}{6} \frac{\text{Tr}(D_j^2)}{N}$.

The minimum energy configuration is

$$D_j = L_j \text{ with } E_0 = -\frac{N^2-1}{24}.$$

The L_j satisfy

$$[L_j, L_k] = i\epsilon_{jkl}L_l \text{ and } L_j L_j = \frac{N^2-1}{4} \mathbf{1}.$$

These are the familiar commutation relations of angular momentum.

One can couple the model to Fermions. Consider the Dirac operator

$$\mathcal{D} = \sigma_j[D_j, \cdot] + 1 ,$$

with $\mathcal{D}\Psi = \sigma_j[D_j, \Psi] + \Psi$.

Then one can see the ground state geometry via the “spectral triple” $(\mathcal{H}, Mat_N, \mathcal{D}_0)$, where the algebra is Mat_N with trace norm and

$$\mathcal{D}_0 = \sigma_a[L_a, \cdot] + 1.$$

This Dirac operator has the same spectrum as that of the commutative sphere but with a cutoff at high energies.

The ground state geometry is that of a fuzzy sphere.

One can couple the model to Fermions. Consider the Dirac operator

$$\mathcal{D} = \sigma_j[D_j, \cdot] + 1 ,$$

with $\mathcal{D}\Psi = \sigma_j[D_j, \Psi] + \Psi$.

Then one can see the ground state geometry via the “spectral triple” $(\mathcal{H}, Mat_N, \mathcal{D}_0)$, where the algebra is Mat_N with trace norm and

$$\mathcal{D}_0 = \sigma_a[L_a, \cdot] + 1.$$

This Dirac operator has the same spectrum as that of the commutative sphere but with a cutoff at high energies. The ground state geometry is that of a fuzzy sphere.

One can couple the model to Fermions. Consider the Dirac operator

$$\mathcal{D} = \sigma_j[D_j, \cdot] + 1 ,$$

with $\mathcal{D}\Psi = \sigma_j[D_j, \Psi] + \Psi$.

Then one can see the ground state geometry via the “spectral triple” $(\mathcal{H}, Mat_N, \mathcal{D}_0)$, where the algebra is Mat_N with trace norm and

$$\mathcal{D}_0 = \sigma_a[L_a, \cdot] + 1.$$

This Dirac operator has the same spectrum as that of the commutative sphere but with a cutoff at high energies.

The ground state geometry is that of a fuzzy sphere.

One can couple the model to Fermions. Consider the Dirac operator

$$\mathcal{D} = \sigma_j[D_j, \cdot] + 1 ,$$

with $\mathcal{D}\Psi = \sigma_j[D_j, \Psi] + \Psi$.

Then one can see the ground state geometry via the “spectral triple” $(\mathcal{H}, Mat_N, \mathcal{D}_0)$, where the algebra is Mat_N with trace norm and

$$\mathcal{D}_0 = \sigma_a[L_a, \cdot] + 1.$$

This Dirac operator has the same spectrum as that of the commutative sphere but with a cutoff at high energies. The ground state geometry is that of a fuzzy sphere.

A sphere from matrices

$$\text{Let } N_j = \frac{2}{\sqrt{N^2-1}} L_j$$

We get a sphere

$$N_1^2 + N_2^2 + N_3^2 = 1. \quad \text{A nice round sphere.}$$

But it is non-commutative.

$$[N_1, N_2] = \frac{2i}{\sqrt{N^2-1}} N_3$$

There is an uncertainty principle for spatial position!

But for $N \rightarrow \infty$ we recover a commutative sphere.

A sphere from matrices

$$\text{Let } N_j = \frac{2}{\sqrt{N^2-1}} L_j$$

We get a sphere

$$N_1^2 + N_2^2 + N_3^2 = \mathbf{1}. \quad \text{A nice round sphere.}$$

But it is non-commutative.

$$[N_1, N_2] = \frac{2i}{\sqrt{N^2-1}} N_3$$

There is an uncertainty principal for spatial position!

But for $N \rightarrow \infty$ we recover a commutative sphere.

A sphere from matrices

$$\text{Let } N_j = \frac{2}{\sqrt{N^2-1}} L_j$$

We get a sphere

$$N_1^2 + N_2^2 + N_3^2 = \mathbf{1}. \quad \text{A nice round sphere.}$$

But it is non-commutative.

$$[N_1, N_2] = \frac{2i}{\sqrt{N^2-1}} N_3$$

There is an uncertainty principal for spatial position!

But for $N \rightarrow \infty$ we recover a commutative sphere.

A sphere from matrices

$$\text{Let } N_j = \frac{2}{\sqrt{N^2-1}} L_j$$

We get a sphere

$$N_1^2 + N_2^2 + N_3^2 = \mathbf{1}. \quad \text{A nice round sphere.}$$

But it is non-commutative.

$$[N_1, N_2] = \frac{2i}{\sqrt{N^2-1}} N_3$$

There is an uncertainty principal for spatial position!

But for $N \rightarrow \infty$ we recover a commutative sphere.

A sphere from matrices

$$\text{Let } N_j = \frac{2}{\sqrt{N^2-1}} L_j$$

We get a sphere

$$N_1^2 + N_2^2 + N_3^2 = \mathbf{1}. \quad \text{A nice round sphere.}$$

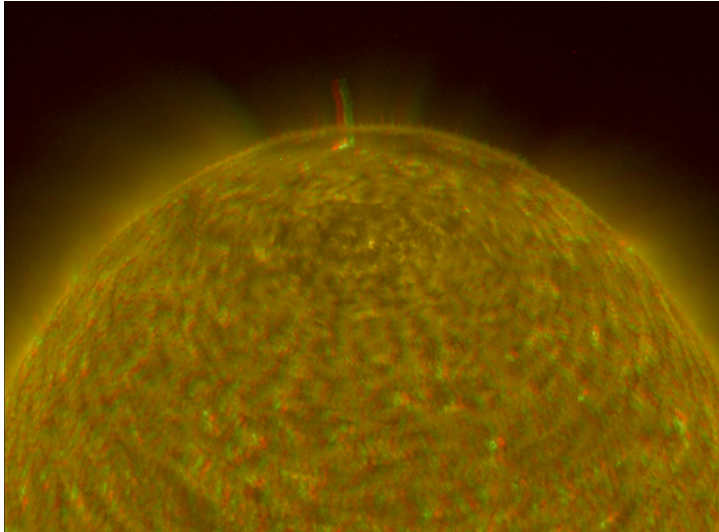
But it is non-commutative.

$$[N_1, N_2] = \frac{2i}{\sqrt{N^2-1}} N_3$$

There is an uncertainty principal for spatial position!

But for $N \rightarrow \infty$ we recover a commutative sphere.

Our “fuzzy” sphere



A 3-matrix model with “matter”.

Adding a scalar field to the model with energy

$$E_{matter}[D, \Phi] = \frac{\text{Tr}}{N} (-a[D_j, \Phi]^2 + b\Phi^2 + c\Phi^4)$$

The complete model is now

$$S[D, \Phi] = \beta \frac{\text{Tr}}{N} \left(-\frac{1}{4} [D_j, D_k]^2 + \frac{2i}{3} \epsilon_{jkl} D_j D_k D_l - a[D_j, \Phi]^2 + b\Phi^2 + c\Phi^4 \right)$$

The ground state $D_j = L_j$ provides a background geometry for the matter.

A 3-matrix model with “matter”.

Adding a scalar field to the model with energy

$$E_{matter}[D, \Phi] = \frac{Tr}{N}(-a[D_j, \Phi]^2 + b\Phi^2 + c\Phi^4)$$

The complete model is now

$$S[D, \Phi] = \beta \frac{Tr}{N} \left(-\frac{1}{4}[D_j, D_k]^2 + \frac{2i}{3}\epsilon_{jkl} D_j D_k D_l - a[D_j, \Phi]^2 + b\Phi^2 + c\Phi^4 \right)$$

The ground state $D_j = L_j$ provides a background geometry for the matter.

A fuzzy field theory model.

Fuzzy field theories are matrix models with fixed background matrices. The scalar field theory on the fuzzy sphere is then :

$$S_N(\Phi, a, b, c) = \text{Tr}(-a[L_j, \Phi]^2 + b\Phi^2 + c\Phi^4)$$

L_j are the generators of $su(2)$ in the N dimensional representation. again with Φ an $N \times N$ matrix. The action $S_N(\Phi, a, b, c)$ converges for $N \rightarrow \infty$ to the action of a scalar field ϕ on the round commutative sphere

$$S(\phi, r, \lambda) = \int_{S^2} d^2x \sqrt{g} \left(\frac{1}{2} \partial_\mu \phi \partial^\mu \phi + \frac{r}{2} \phi^2 + \frac{\lambda}{4!} \phi^4 \right).$$

$$\lim_{N \rightarrow \infty} \left| S(\phi, r, \lambda) - S_N\left(\Phi, \frac{1}{2N}, \frac{r}{2N}, \frac{\lambda}{4!N}\right) \right| \rightarrow 0.$$

The matrix $\Phi = \int_{S^2} \omega \rho_N \phi$, with ω the unit volume form on S^2 and ρ_N is a particular matrix valued function on S^2 .

$$\rho_N = \sum_{lm} Y_{lm} \hat{Y}_{lm}$$

where Y_{lm} are the spherical harmonics and \hat{Y}_{lm} are polarization tensors satisfying

$$[L_3, \hat{Y}_{lm}] = m \hat{Y}_{lm} \quad \text{and} \quad [L_j, [L_j, \hat{Y}_{lm}]] = l(l+1) \hat{Y}_{lm} .$$

So that if

$$\phi = \sum_{l=0}^{\infty} \sum_{m=-l}^l c_{lm} Y_{lm}$$

then

$$\Phi = \sum_{l=0}^{N-1} \sum_{m=-l}^l c_{lm} \hat{Y}_{lm}$$

The matrix $\Phi = \int_{S^2} \omega \rho_N \phi$, with ω the unit volume form on S^2 and ρ_N is a particular matrix valued function on S^2 .

$$\rho_N = \sum_{lm} Y_{lm} \hat{Y}_{lm}$$

where Y_{lm} are the spherical harmonics and \hat{Y}_{lm} are polarization tensors satisfying

$$[L_3, \hat{Y}_{lm}] = m \hat{Y}_{lm} \quad \text{and} \quad [L_j, [L_j, \hat{Y}_{lm}]] = l(l+1) \hat{Y}_{lm} .$$

So that if

$$\phi = \sum_{l=0}^{\infty} \sum_{m=-l}^l c_{lm} Y_{lm}$$

then

$$\Phi = \sum_{l=0}^{N-1} \sum_{m=-l}^l c_{lm} \hat{Y}_{lm}$$

Small fluctuations

The zero temperature ground state of the model

$$E = \frac{Tr}{N} \left(-\frac{1}{4} [D_j, D_k]^2 + \frac{2i}{3} \epsilon_{jkl} D_j D_k D_l \right)$$

is a round fuzzy sphere with $D_j = L_j$ and $E_0 = -\frac{L_j^2}{6}$.

Expanding around the minimum solution, $D_j = L_j + A_j$ yields a noncommutative Yang-Mills action with field strength

$$F_{jk} = i[L_j, A_k] - i[L_j, A_k] + \epsilon_{jkl} A_l + i[A_j, A_b k].$$

As written the gauge field includes a scalar field,

$$\Phi = \frac{1}{\sqrt{N^2-1}} (D_j - L_j)^2 = \frac{1}{2} (N_j A_j + A_j N_j + \frac{A_j^2}{\sqrt{c_2}}).$$

It is the component of the gauge field normal to the sphere when viewed as imbedded in \mathbf{R}^3 with $N_j = \frac{L_j}{\sqrt{c_2}}$ and $c_2 = L_j^2 = (N^2 - 1)/4$.

Small fluctuations

The zero temperature ground state of the model

$$E = \frac{\text{Tr}}{N} \left(-\frac{1}{4} [D_j, D_k]^2 + \frac{2i}{3} \epsilon_{jkl} D_j D_k D_l \right)$$

is a round fuzzy sphere with $D_j = L_j$ and $E_0 = -\frac{L_j^2}{6}$.

Expanding around the minimum solution, $D_j = L_j + A_j$ yields a noncommutative Yang-Mills action with field strength

$$F_{jk} = i[L_j, A_k] - i[L_j, A_k] + \epsilon_{jkl} A_l + i[A_j, A_k].$$

As written the gauge field includes a scalar field,

$$\Phi = \frac{1}{\sqrt{N^2-1}} (D_j - L_j)^2 = \frac{1}{2} (N_j A_j + A_j N_j + \frac{A_j^2}{\sqrt{c_2}}).$$

It is the component of the gauge field normal to the sphere when viewed as imbedded in \mathbf{R}^3 with $N_j = \frac{L_j}{\sqrt{c_2}}$ and $c_2 = L_j^2 = (N^2 - 1)/4$.

Small fluctuations

The zero temperature ground state of the model

$$E = \frac{Tr}{N} \left(-\frac{1}{4} [D_j, D_k]^2 + \frac{2i}{3} \epsilon_{jkl} D_j D_k D_l \right)$$

is a round fuzzy sphere with $D_j = L_j$ and $E_0 = -\frac{L_j^2}{6}$.

Expanding around the minimum solution, $D_j = L_j + A_j$ yields a noncommutative Yang-Mills action with field strength

$$F_{jk} = i[L_j, A_k] - i[L_j, A_k] + \epsilon_{jkl} A_l + i[A_j, A_k].$$

As written the gauge field includes a scalar field,

$$\Phi = \frac{1}{\sqrt{N^2-1}} (D_j - L_j)^2 = \frac{1}{2} (N_j A_j + A_j N_j + \frac{A_j^2}{\sqrt{c_2}}).$$

It is the component of the gauge field normal to the sphere when viewed as imbedded in \mathbf{R}^3 with $N_j = \frac{L_j}{\sqrt{c_2}}$ and $c_2 = L_j^2 = (N^2 - 1)/4$.

Small fluctuations

The zero temperature ground state of the model

$$E = \frac{\text{Tr}}{N} \left(-\frac{1}{4} [D_j, D_k]^2 + \frac{2i}{3} \epsilon_{jkl} D_j D_k D_l \right)$$

is a round fuzzy sphere with $D_j = L_j$ and $E_0 = -\frac{L_j^2}{6}$.

Expanding around the minimum solution, $D_j = L_j + A_j$ yields a noncommutative Yang-Mills action with field strength

$$F_{jk} = i[L_j, A_k] - i[L_j, A_k] + \epsilon_{jkl} A_l + i[A_j, A_k].$$

As written the gauge field includes a scalar field,

$$\Phi = \frac{1}{\sqrt{N^2-1}} (D_j - L_j)^2 = \frac{1}{2} (N_j A_j + A_j N_j + \frac{A_j^2}{\sqrt{c_2}}).$$

It is the component of the gauge field normal to the sphere when viewed as imbedded in \mathbf{R}^3 with $N_j = \frac{L_j}{\sqrt{c_2}}$ and $c_2 = L_j^2 = (N^2 - 1)/4$.

Small fluctuations

The zero temperature ground state of the model

$$E = \frac{T_r}{N} \left(-\frac{1}{4} [D_j, D_k]^2 + \frac{2i}{3} \epsilon_{jkl} D_j D_k D_l \right)$$

is a round fuzzy sphere with $D_j = L_j$ and $E_0 = -\frac{L_j^2}{6}$.

Expanding around the minimum solution, $D_j = L_j + A_j$ yields a noncommutative Yang-Mills action with field strength

$$F_{jk} = i[L_j, A_k] - i[L_j, A_k] + \epsilon_{jkl} A_l + i[A_j, A_b k].$$

As written the gauge field includes a scalar field,

$$\Phi = \frac{1}{\sqrt{N^2-1}} (D_j - L_j)^2 = \frac{1}{2} (N_j A_j + A_j N_j + \frac{A_j^2}{\sqrt{c_2}}).$$

It is the component of the gauge field normal to the sphere when viewed as imbedded in \mathbf{R}^3 with $N_j = \frac{L_j}{\sqrt{c_2}}$ and $c_2 = L_j^2 = (N^2 - 1)/4$.

Larger context

The model can be obtained by reduction of $\mathcal{N} = 4$ SUSY Yang-Mills or equivalently from the ADS/CFT corresponding situation. Or from $d = 11$ supergravity.

An intermediate model in all of these reductions is the Berenstein, Maldacena, Nastase matrix model.

In fact this procedure gives a higherarchy of additional models currently under study.

Larger context

The model can be obtained by reduction of $\mathcal{N} = 4$ SUSY Yang-Mills or equivalently from the ADS/CFT corresponding situation. Or from $d = 11$ supergravity.

An intermediate model in all of these reductions is the Berenstein, Maldacena, Nastase matrix model.

In fact this procedure gives a hierarchy of additional models currently under study.

Larger context

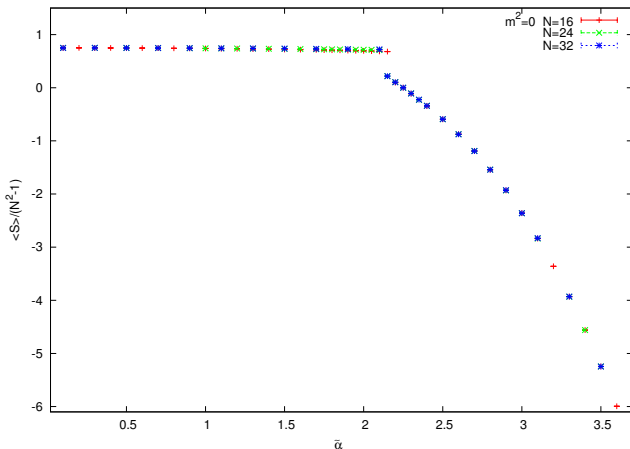
The model can be obtained by reduction of $\mathcal{N} = 4$ SUSY Yang-Mills or equivalently from the ADS/CFT corresponding situation. Or from $d = 11$ supergravity.

An intermediate model in all of these reductions is the Berenstein, Maldacena, Nastase matrix model.

In fact this procedure gives a higherarchy of additional models currently under study.

Increasing the temperature. Monte Carlo Simulations

The singular part of the entropy is given by \mathcal{S}/N^2 where $\mathcal{S} = \langle S \rangle$ and $\beta = \tilde{\alpha}^4$



The entropy jump

$\mathcal{S} = \frac{5}{12}$ as the transition is approached from the fuzzy sphere side,

and jumps to $\mathcal{S} = \frac{3}{4}$ in the high temperature phase.

The infinite temperature entropy does not contribute $\frac{1}{2}$ but $\frac{1}{4}$ per degree of freedom.

So the model remains highly interacting at high temperatures.

The entropy jump

$\mathcal{S} = \frac{5}{12}$ as the transition is approached from the fuzzy sphere side,

and jumps to $\mathcal{S} = \frac{3}{4}$ in the high temperature phase.

The infinite temperature entropy does not contribute $\frac{1}{2}$ but $\frac{1}{4}$ per degree of freedom.

So the model remains highly interacting at high temperatures.

The entropy jump

$\mathcal{S} = \frac{5}{12}$ as the transition is approached from the fuzzy sphere side,

and jumps to $\mathcal{S} = \frac{3}{4}$ in the high temperature phase.

The infinite temperature entropy does not contribute $\frac{1}{2}$ but $\frac{1}{4}$ per degree of freedom.

So the model remains highly interacting at high temperatures.

The entropy jump

$\mathcal{S} = \frac{5}{12}$ as the transition is approached from the fuzzy sphere side,

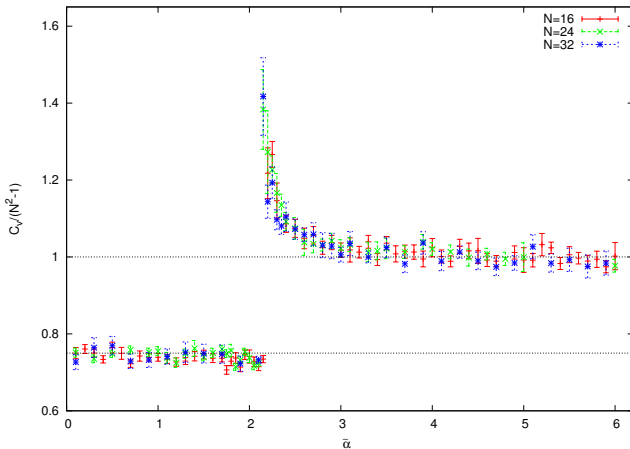
and jumps to $\mathcal{S} = \frac{3}{4}$ in the high temperature phase.

The infinite temperature entropy does not contribute $\frac{1}{2}$ but $\frac{1}{4}$ per degree of freedom.

So the model remains highly interacting at high temperatures.

Specific Heat

The specific heat C_v/N^2 where $C_v = \langle S^2 \rangle - \langle S \rangle^2$ and



$$\beta = \tilde{\alpha}^4$$

Specific Heat Exponent

Entropy Jump

The transition is unusual in that it has a jump in the entropy.

$\Delta S = \frac{1}{3}$ indicating a 1st order transition.

Divergent Specific Heat

But it has a divergent specific heat $C = A_-(T_c - T)^{-\alpha}$ typical of a continuous (or second order) transition. We find the specific heat exponent $\alpha = \frac{1}{2}$.

Our analysis gives the critical point $\beta_c = (\frac{8}{3})^3$ and a critical exponent $\alpha = \frac{1}{2}$ for the divergence of the specific heat.

Specific Heat Exponent

Entropy Jump

The transition is unusual in that it has a jump in the entropy.

$\Delta S = \frac{1}{3}$ indicating a 1st order transition.

Divergent Specific Heat

But it has a divergent specific heat $C = A_-(T_c - T)^{-\alpha}$ typical of a continuous (or second order) transition. We find the specific heat exponent $\alpha = \frac{1}{2}$.

Our analysis gives the critical point $\beta_c = (\frac{8}{3})^3$ and a critical exponent $\alpha = \frac{1}{2}$ for the divergence of the specific heat.

Specific Heat Exponent

Entropy Jump

The transition is unusual in that it has a jump in the entropy.

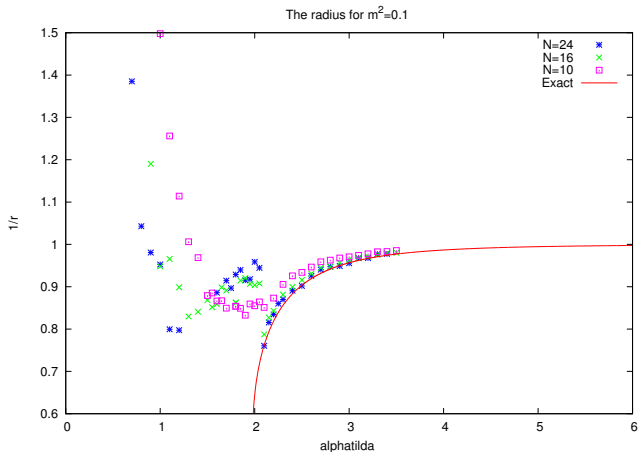
$\Delta S = \frac{1}{3}$ indicating a 1st order transition.

Divergent Specific Heat

But it has a divergent specific heat $C = A_-(T_c - T)^{-\alpha}$ typical of a continuous (or second order) transition. We find the specific heat exponent $\alpha = \frac{1}{2}$.

Our analysis gives the critical point $\beta_c = \left(\frac{8}{3}\right)^3$ and a critical exponent $\alpha = \frac{1}{2}$ for the divergence of the specific heat.

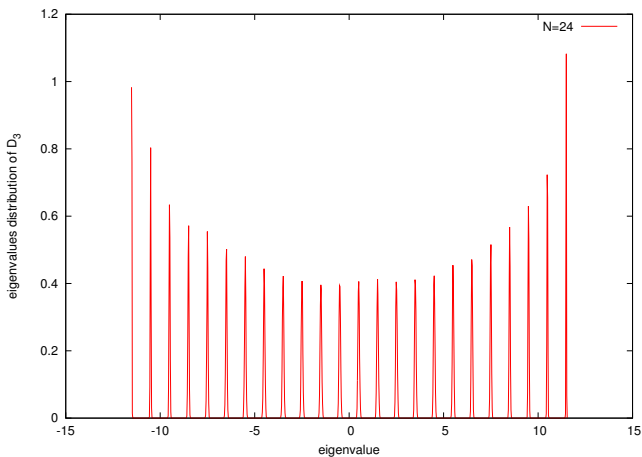
As the temperature is increased the fuzzy sphere expands and evaporates





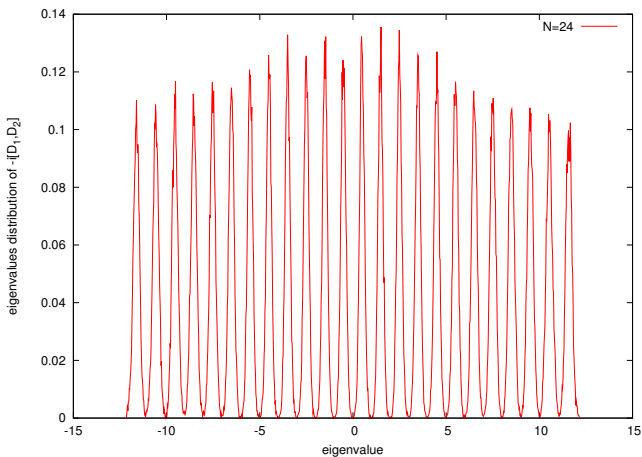
Eigenvalues in the low temperature phase

Eigenvalue distribution of D_3 for $N = 24$.



Eigenvalues in the low temperature phase

Eigenvalue distribution of $[D_1, D_2]$ for $N = 24$.



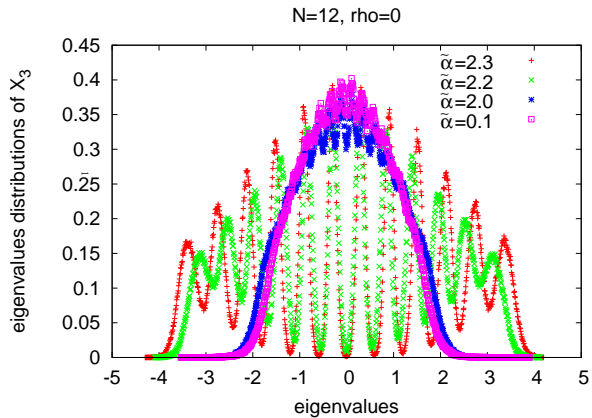
A closer look at the transition

- In the fuzzy sphere phase the eigenvalues fluctuate around the discrete values corresponding to $D_a = L_a$, the irreducible representation of $SU(2)$ of dimension N .
- In the matrix phase, the distribution of eigenvalues of

$$X_a = \left(\frac{\beta}{N^2}\right)^{1/4} D_a = \frac{\tilde{\alpha}}{N^{1/2}} D_a$$

is largely independent of $\tilde{\alpha}$ and of N .

- In fact fluctuations are around commuting matrices with a uniform distribution in a ball of radius 2. E.g for $N = 12$, the distribution for X_3 ranges from -2 to 2 .

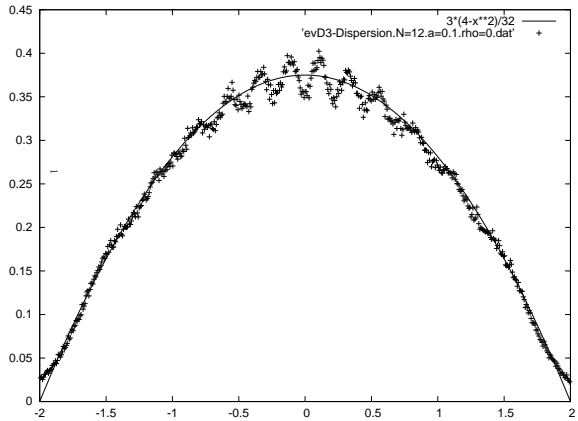


- Following Berenstein et al. (arXiv:0805.4658) one can expand small fluctuations around commuting diagonal matrices. This leads to the conclusion that the eigenvalues form a solid ball of radius R .

The distribution of eigenvalues of X_3 is then:

$$\rho(x) = \frac{3}{4R^3}(R^2 - x^2)$$

This implies $\langle x^2 \rangle = \frac{R^2}{5}$. Numerically, $R \approx 2$.



From solid ball of eigenvalues to fuzzy S^2 .

As the system cools a fuzzy S^2 emerges from the ball corresponding to the eigenvalues of the commuting matrices at high temperature.

In passing through the transition the eigenvalue ball of radius 2 expands to a fuzzy sphere of radius $\frac{\sqrt{N}\tilde{\alpha}}{2}$.

Conclusions

- We have we a good understanding of the 3-matrix model. It provides a concrete model where one can track the geometry as it passes through a phase transition and dissapears.
Such transitions belong to a new universality class of topological phase transitions.
- The transition is is in the geometry. The underlying geometry at a microscopic level is non-commutative— described by a fuzzy sphere with matter fluctuations. At high temperatures the eigenvalues form a solid ball of infinitesimal radius on the scale of the fuzzy sphere.
- The geometrical phase emerges as the system cools. This is suggestive of a geometrical phase emerging as the universe cools, or perhaps as the relevant coupling runs to a larger scale.
- The fluctuations around the fuzzy sphere phase are consistent with being $U(1)$ gauge fields in the large mass limit.

Conclusions

- We have we a good understanding of the 3-matrix model. It provides a concrete model where one can track the geometry as it passes through a phase transition and disappears. *Such transitions belong to a new universality class of topological phase transitions.*
- The transition is is in the geometry. The underlying geometry at a microscopic level is non-commutative— described by a fuzzy sphere with matter fluctuations. At high temperatures the eigenvalues form a solid ball of infinitesimal radius on the scale of the fuzzy sphere.
- The geometrical phase emerges as the system cools. This is suggestive of a geometrical phase emerging as the universe cools, or perhaps as the relevant coupling runs to a larger scale.
- The fluctuations around the fuzzy sphere phase are consistent with being $U(1)$ gauge fields in the large mass limit.

Conclusions

- We have we a good understanding of the 3-matrix model. It provides a concrete model where one can track the geometry as it passes through a phase transition and disappears.
Such transitions belong to a new universality class of topological phase transitions.
- The transition is is in the geometry. The underlying geometry at a microscopic level is non-commutative— described by a fuzzy sphere with matter fluctuations. At high temperatures the eigenvalues form a solid ball of infinitesimal radius on the scale of the fuzzy sphere.
- The geometrical phase emerges as the system cools. This is suggestive of a geometrical phase emerging as the universe cools, or perhaps as the relevant coupling runs to a larger scale.
- The fluctuations around the fuzzy sphere phase are consistent with being $U(1)$ gauge fields in the large mass limit.

Conclusions

- We have we a good understanding of the 3-matrix model. It provides a concrete model where one can track the geometry as it passes through a phase transition and disappears. *Such transitions belong to a new universality class of topological phase transitions.*
- The transition is is in the geometry. The underlying geometry at a microscopic level is non-commutative— described by a fuzzy sphere with matter fluctuations. At high temperatures the eigenvalues form a solid ball of infinitesimal radius on the scale of the fuzzy sphere.
- The geometrical phase emerges as the system cools. This is suggestive of a geometrical phase emerging as the universe cools, or perhaps as the relevant coupling runs to a larger scale.
- The fluctuations around the fuzzy sphere phase are consistent with being $U(1)$ gauge fields in the large mass limit.

Conclusions

- We have we a good understanding of the 3-matrix model. It provides a concrete model where one can track the geometry as it passes through a phase transition and disappears. *Such transitions belong to a new universality class of topological phase transitions.*
- The transition is is in the geometry. The underlying geometry at a microscopic level is non-commutative— described by a fuzzy sphere with matter fluctuations. At high temperatures the eigenvalues form a solid ball of infinitesimal radius on the scale of the fuzzy sphere.
- The geometrical phase emerges as the system cools. This is suggestive of a geometrical phase emerging as the universe cools, or perhaps as the relevant coupling runs to a larger scale.
- The fluctuations around the fuzzy sphere phase are consistent with being $U(1)$ gauge fields in the large mass limit.

Thank you for your attention!